Parameter Identification in Cyclic Voltammetry
of Alkaline Methanol Oxidation

Tanja Clees[1], Igor Nikitin[1], Lialia Nikitina[1], Sabine Pott[1], Ulrike Krewer[2] and Theresa Haisch[2]

[1]*Fraunhofer Institute for Algorithms and Scientific Computing, Sankt Augustin, Germany*

[2]*Institute of Energy and Process Systems Engineering, Technical University Braunschweig, Germany*

Abstract: Alkaline methanol oxidation is an electrochemical process, perspective for the design of efficient high energy density fuel cells. The process involves a large number of elementary reactions, forming a complex reaction graph, and it is described by a system of non-linear differential equations of high order. The purpose of parameter identification is a reconstruction of reaction constants in this model on the basis of available experimental data. Cyclic voltammetry, a measurement of dynamical current-voltage characteristic of the cell, is especially suitable for analysis of electrochemical kinetics. In this paper we present several approaches for parameter identification in cyclic voltammetry of alkaline methanol oxidation. With the aid of global optimization methods and interactive parameter study we find four islands of solutions in parameter space, corresponding to different chemical mechanisms of the process. The main features of solutions are discussed and the reconstructed reaction constants are presented.

1 INTRODUCTION

Direct fuel cells are attractive portable energy sources, serving as converters of chemical energy to the electric one, with a possibility to refill the reagents. Alkaline methanol oxidation uses commonly available components and allows to reduce the costs for production and operation of the cells. The detailed description of this chemical process includes a large number of reactions, multiple intermediates, leading to a mathematical model with many unknown parameters (Krewer et al., 2011; Krewer et al., 2006; Beden et al., 1982).

For parameter identification different types of experiments are used (Ciucci, 2013; Gamry Instruments, 2018). Some of them measure stationary current-voltage profiles of the cell, others use a linearization near the stationary point and scan a response of the cell to harmonic oscillations in a large range of frequencies. In our previous paper (Clees et al., 2017) we have presented the methods for parameter identification in this type of measurements. The main difficulty here is that the stationary state in the considered process is hard to reach experimentally. Our laboratory measurements show that even if one leaves the cell under fixed voltage for six hours, it

does not reach a steady current. A presumable reason is a gradual poisoning of the electrode with intermediates or byproducts of reactions, characteristic for the measurements of this type.

In this paper, differently from (Clees et al., 2017), the measurement method is used, not assuming the presence of the stationary state. Cyclic voltammetry (Bard and Faulkner, 2000) is an experimental setup, where the cell is subjected to a saw-like voltage variation of high amplitude. These voltage variations clean up the electrode during every period, in this way preventing the electrode poisoning. On the side of parameter identification, however, the problem becomes more difficult, since one needs to integrate numerically stiff non-linear differential equations, instead of just testing the linear response of the system.

In general, parameter identification uses a version of non-linear least square method (Press et al., 1992; Strutz, 2016) to fit the experimental data with the mathematical model. One can also take into account any equality or inequality constraints by the methods of non-linear programming, e.g., interior point method (Wächter and Biegler, 2006). These methods find only a local optimum and should be enhanced by global strategies to find all relevant solutions. One possibility is an interactive exploration of solution

279
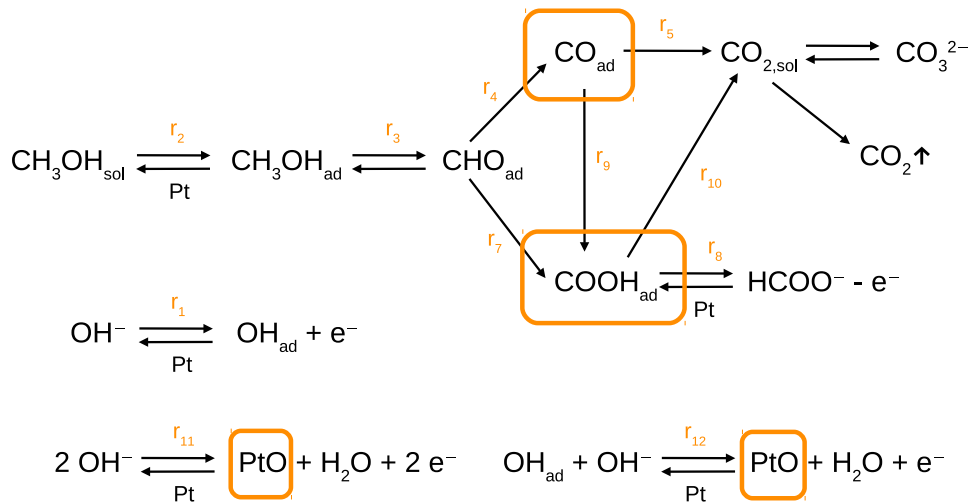
Figure 1: Reaction graph. Orange frames indicate possible locations of weakly coupled reagents.

Table 1: Numeration of variables and constants.

Variables		Constants	
θ_1	OH_{ad}		
θ_2	CH_3OH_{ad}	c_1	OH^-
θ_3	CHO_{ad}	c_2	CH_3OH
θ_4	CO_{ad}	c_3	H_2O
θ_5	$COOH_{ad}$		
θ_6	PtO		

Table 2: Model constants.

Constant, units	Value
F, C/mol	$9.649 \cdot 10^4$
R, J/(K mol)	8.314
A, m^2	$2.376 \cdot 10^{-5}$
C_{dl}, F	$1.899 \cdot 10^{-4}$
C_{act}, mol/m^2	$8.523 \cdot 10^{-5}$
α	0.5

space using metamodeling with radial basis functions (Nikitin et al., 2012; Clees et al., 2014a; Clees et al., 2014b). For the problem in hand, however, solutions occupy thin subsets of parameter space. Also, the dependence of model response on parameters includes rapidly growing exponential terms, too non-linear to be caught with radial basis functions. Instead of interpolating the response, one can directly solve the differential equations, provided that the integrator is sufficiently fast. Interactive exploration can be also enhanced with standard global optimization methods (Bäck, 1996; Ilonen et al., 2003; Otten and van Ginneken, 1989), including genetic algorithms, differential evolution, simulated annealing, etc.

In this paper we use a combination of automatic global methods and interactive parameter study. In Section 2 we present the mathematical model behind alkaline methanol oxidation. In Section 3 the experimental measurements are described. In Section 4 the details on parameter identification methods are given. Section 5 presents the obtained results.

2 ALKALINE METHANOL OXIDATION

Considering alkaline methanol oxidation processes, we use the list of reactions from our previous work (Clees et al., 2017):

r_1: $OH^- + Pt \leftrightarrow OH_{ad} + e^-$
r_2: $CH_3OH + Pt \leftrightarrow CH_3OH_{ad}$
r_3: $CH_3OH_{ad} + 3OH_{ad} \leftrightarrow CHO_{ad} + 3H_2O$
r_4: $CHO_{ad} + OH_{ad} \rightarrow CO_{ad} + H_2O$
r_5: $CO_{ad} + 2OH_{ad} \rightarrow CO_2 + H_2O + 2Pt$
r_7: $CHO_{ad} + 2OH_{ad} \rightarrow COOH_{ad} + H_2O + Pt$
r_8: $COOH_{ad} + e^- \leftrightarrow HCOO^- + Pt$
r_9: $CO_{ad} + OH_{ad} \rightarrow COOH_{ad} + Pt$
r_{10}: $COOH_{ad} + OH_{ad} \rightarrow CO_2 + H_2O + 2Pt$
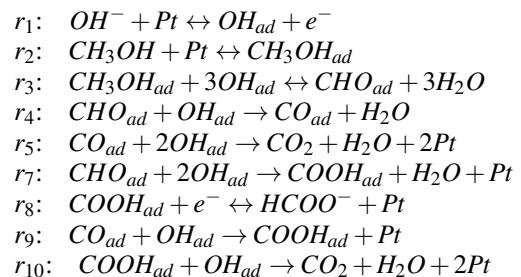
extending it with two additional reactions:

r_{11}: $2OH^- + Pt \leftrightarrow PtO + H_2O + 2e^-$
r_{12}: $OH^- + OH_{ad} \leftrightarrow PtO + H_2O + e^-$
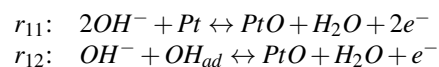
Fig. 1 schematically represents the reactions. The mathematical model for these processes is formulated as follows. The reagents adsorbed on the electrode (subscript "ad") are represented by surface coverage variables θ_{1-6}, while the reagents in the solvent are represented by constant mole fractions values c_{1-3}. The assignment of the reagents is given in Table 1.

Counting the factors of the reagents in the reactions, one forms molar and charge balance conditions:

$$
\begin{aligned}
F_1 &= (r_1 - 3r_3 - r_4 - 2r_5 - 2r_7 \\
&\quad - r_9 - r_{10} - r_{12})/C_{act}, \\
F_2 &= (r_2 - r_3)/C_{act}, \\
F_3 &= (r_3 - r_4 - r_7)/C_{act}, \\
F_4 &= (r_4 - r_5 - r_9)/C_{act}, \\
F_5 &= (r_7 - r_8 + r_9 - r_{10})/C_{act}, \\
F_6 &= (r_{11} + r_{12})/C_{act}, \\
F_7 &= (-r_1 + r_8 - 2r_{11} - r_{12}) \cdot FA/C_{dl},
\end{aligned}
\tag{1}
$$

where r_i are reaction rates, F_i are production rates, F_{1-6} – for adsorbed reagents, F_7 – for electrons. The constants, participating in these equations, are: C_{act} – surface concentration of catalyst, F – Faraday constant, A – geometric electrode area, C_{dl} – cell capacitance.

Reaction rates are described by a kinetic model:

$$
\begin{aligned}
r_1 &= k_1 c_1 \theta_0 - k_{-1}\theta_1, \quad r_2 = k_2 c_2 \theta_0 - k_{-2}\theta_2, \\
r_3 &= k_3 \theta_2 \theta_1^3 - k_{-3}\theta_3 c_3^3, \quad r_4 = k_4 \theta_3 \theta_1, \\
r_5 &= k_5 \theta_4 \theta_1^2, \quad r_7 = k_7 \theta_3 \theta_1^2, \quad r_8 = k_8 \theta_5, \\
r_9 &= k_9 \theta_4 \theta_1, \quad r_{10} = k_{10} \theta_5 \theta_1, \\
r_{11} &= k_{11} c_1^2 \theta_0 - k_{-11} c_3 \theta_6, \\
r_{12} &= k_{12} c_1 \theta_1 - k_{-12} c_3 \theta_6,
\end{aligned}
\tag{2}
$$

where k_i are reaction constants. The model directly encodes molecular reactions in terms of probabilities of collision, e.g., in reaction r_5, the term $\theta_4\theta_1^2$ corresponds to a probability, that one *CO*-particle meets two *OH*-particles. The variable θ_0 describes non-covered surface of the electrode. The variables θ_i are changed in the range $[0,1]$ with summation rule $\sum_0^6 \theta_i = 1$. The constants for the reactions, involving electrons, are defined by Tafel equation:

$$
\begin{aligned}
k_1 &= k_1^0 \exp(\alpha\beta\eta), \\
k_{-1} &= k_{-1}^0 \exp(-(1-\alpha)\beta\eta), \\
k_8 &= k_8^0 \exp(-(1-\alpha)\beta\eta), \quad \beta = F/(RT), \\
k_{11} &= k_{11}^0 \exp(2\alpha\beta\eta), \quad k_{12} = k_{12}^0 \exp(\alpha\beta\eta), \\
k_{-11} &= k_{-11}^0 \exp(-2(1-\alpha)\beta\eta), \\
k_{-12} &= k_{-12}^0 \exp(-(1-\alpha)\beta\eta).
\end{aligned}
\tag{3}
$$

where η is electrode potential, R is universal gas constant, T is absolute temperature, α is charge transfer coefficient. The universal/measured model constants are given in Table 2. The remaining constants, k_i^0 for electrochemical reactions and k_i for other reactions have to be defined by parameter identification procedure. Generally, the constants are constrained only by positivity condition. In our model, reactions r_{11} and r_{12}, describing parallel and sequential mechanism of platinum oxidation, will be considered as alternatives, i.e., we will consider two scenarios with either $k_{\pm 11}^0 = 0$ or $k_{\pm 12}^0 = 0$.

Kinetics of alkaline methanol oxidation is described by a closed system of differential equations:

$$
d\theta_i/dt = F_i(\theta,\eta), \; i = 1 \ldots 6, \tag{4}
$$

where η is considered as a given function of time t. There is an additional equation:

$$
d\eta/dt = F_7(\theta,\eta) + I_{cell}/C_{dl}, \tag{5}
$$

which can be considered as a model prediction for cell current I_{cell}. Comparing it with the measured current values, we can introduce a χ^2-deviation:

$$
\chi^2 = \sum_i (I_{cell,i} - I_{cell,i}^{exp})^2, \tag{6}
$$

which should be minimized in parameter identification procedure.

3 MEASUREMENTS

The measurements are performed in our laboratory in TU Braunschweig. The experiments were done using a three electrode cell setup, shown on Fig.2. It uses a rotating disk electrode (RDE) as a working electrode and a potentiostat. The working electrode was coated with a platinum catalyst ink and an ionomer. A platinum wire was used for the counter electrode and a Hg/HgO electrode as a reference electrode. The potentials were calculated to a normal hydrogen electrode (NHE) as reference. Before each measurement the working electrode was electrochemically cleaned by running CV cycles with the pure electrolyte.

In experiments, different profiles for the voltage $\eta(t)$ are set and the cell current $I_{cell}(t)$ is measured. In particular, constant η profiles correspond to the measurement of *polarization curve* (PC), stepwise $\eta(t)$ is used in *chronoamperometry* (CA). A constant η, perturbed with sinusoidal profile of small amplitude is applied in *electrochemical impedance spectroscopy* (EIS), the same with high amplitude gives the estimation of *total harmonic distortion* (THD).

The measurement of *cyclovoltagramms* (CV) uses saw-like $\eta(t)$ profiles, displayed on Fig.3 left. The resulting $I_{cell}(t)$ profile, a periodic curve, is shown on
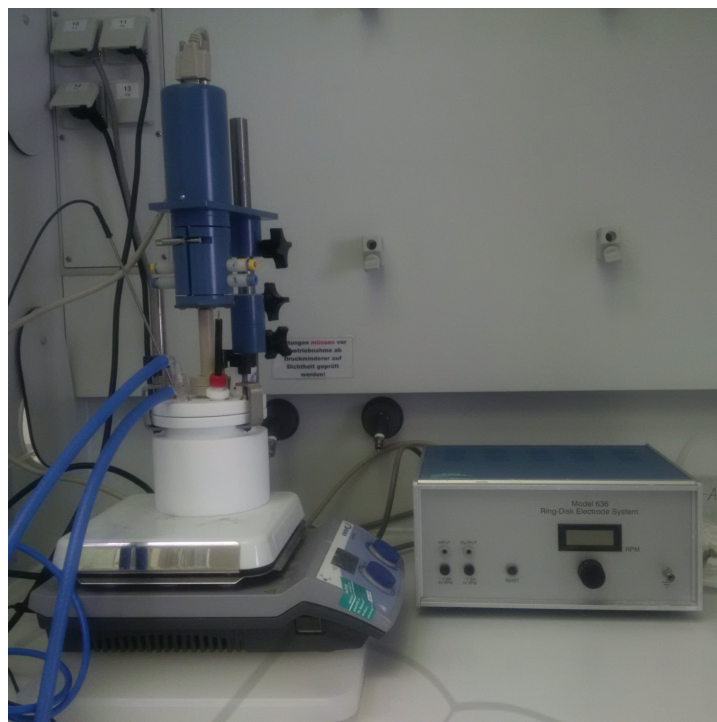
Figure 2: Cyclic voltammetry: experimental setup.
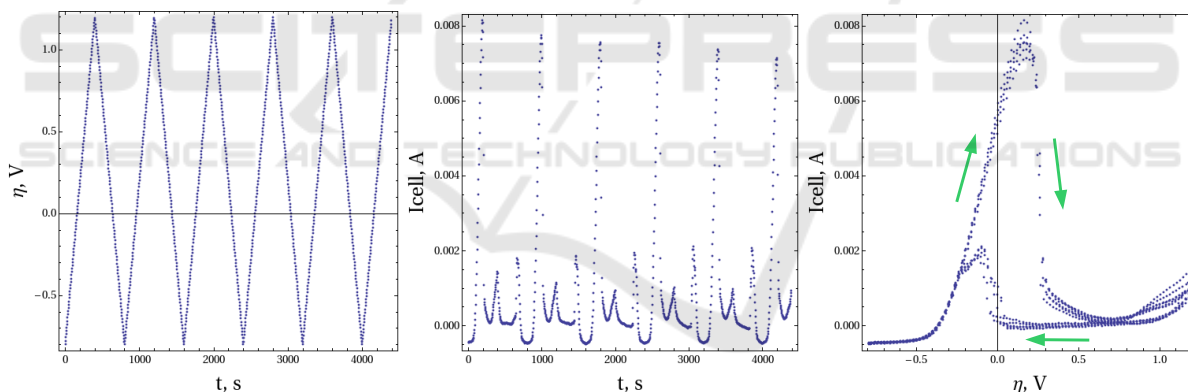
Figure 3: Cyclic voltammetry. From left to right: voltage profile, current profile, current-voltage characteristics with hysteresis effect.

Fig.3 middle. In coordinates (η, I_{cell}) it corresponds to a closed cycle, shown on Fig.3 right. This curve in alkaline methanol oxidation experiments demonstrates a typical *hysteresis* effect, i.e., the path for increasing voltage does not coincide with the decreasing one. The reasons for this effect and the relation with other types of measurements will be discussed below.

Between different measurements, one can also change concentration of the dissolved reagents c_i, the temperature T and the period T_p. In this way one has not a single experiment, but a set of experiments which should be simultaneously fit by the ki-

netic model.

Surface coverage profiles $\theta_i(t)$ are generally not measurable. Although their rough estimation can be done with the aid of Fourier Transform Infrared Spectroscopy (FTIR, (Griffiths and de Hasseth, 2007)), the precision of this approach is not sufficient yet. The usual way to reconstruct the kinetics is the model based parameter identification.

4 PARAMETER IDENTIFICATION

We use *Mathematica* (Mathematica 11, 2018) for analysis of cyclovoltagramms. For solution of the system (4) we use algorithm `NDSolve`, providing a generic, stable and robust numerical integrator of differential equations. The algorithm supports a bundle of methods, both explicit (`ExplicitEuler`, `ExplicitRungeKutta`, `ExplicitMidpoint`) and implicit (`Adams`, `BDF`, `ImplicitRungeKutta`, `SymplecticPartitionedRungeKutta`) ones. Explicit methods require less computational effort per step, but perform more steps to ensure stability. Implicit methods can go in large steps, but each step is computationally expensive. Generally, for stiff systems implicit methods are preferred. The algorithm estimates the stiffness of the system, based on the dominant eigenvalue of the Jacobian. Dependently on this estimation and theoretically known stability regions of the integration methods the algorithm selects a suitable method in respect both to the stability and precision criteria. Precision of the integration is internally estimated by Richardson's formula: $e = |y_2 - y_1|/(2^p - 1)$, where p is the order of the integration method, $|y_2 - y_1|$ is a difference of integration results, performed with a single step h and two sequential half-steps $h/2$. The step is automatically adapted to keep the error estimator just within the absolute and relative tolerance bounds, specified by parameters `AccuracyGoal` and `PrecisionGoal`.

One more convenient feature of `NDSolve` is a possibility to solve both Cauchy initial value problems and boundary problems. We are mainly interested in periodical solutions of the system (4), which can be found by setting linear boundary conditions of the type $x(T_p) = x(0)$. The considered system possesses a polynomial right hand side with periodic coefficients, due to explicit periodical dependence $\eta(t)$, entering in some coefficients. In our numerical experiments, the system rapidly, in one-two periods, converges to a limiting cycle, corresponding to the periodical solution. Therefore, an alternative method is to solve Cauchy initial value problem with an arbitrary starting point, e.g., free electrode $\theta_0 = 1$, and wait some periods till convergence.

For the parameter identification several capabilities of *Mathematica* can be used.

Interactive Parameter Study can be performed with a tool `Manipulate`. It allows to attach interactive manipulators (sliders) to the model parameters, while the results are presented as a collection of plots. The system is reevaluated and the results are replotted every time when the value controlled by the manipulator is changed. Fig.4 shows an example of usage of the interactive manipulators for parameter study in cyclic voltammetry of alkaline methanol oxidation. The manipulators on the left represent reaction coefficients, varied in logarithmic scale in user specified limits. Each manipulator can be opened, revealing additional field with numerical value and a set of buttons for animation and stepwise increments. The current set of parameters is permanently available for the user in a form of a list and can be printed out, exported, etc. with standard commands. The central plot shows a cyclovoltagramm, modeled (red line) vs measured (blue points). The right plot shows a period of evolution for θ values. The ordinal number of reagent is encoded by a color scheme: red, green, blue, cyan, magenta, brown for 1-6 and black for 0, free electrode. The latency of the tool is 0.5 – 1.5 seconds (on 3 GHz CPU), dependently on the number of cyclovoltagramms to evaluate and plots to display. It provides the interactive performance, necessary for parameter study. The tool allows to explore solution space, immediately observing the influence of the parameters, various features and effects in the results (peaks, dips, shifts, etc.) and compare the modeled results with measured data.

Automatic Global Optimization can be done with the algorithm `NMinimize`. It aggregates a collection of derivative free methods, attempting to find a global minimum of a given objective function in a domain, specified by a set of equality and inequality constraints. It is commonly known, that global optimization is a computationally hard task, especially for non-linear multidimensional problems. An additional difficulty in our case is that optimization parameters, reaction constants, in logarithmic scale do not have *a priori* specified limits. Exponential terms in the equations can change their contribution by dozens of orders, also the constants are multiplied by coverage values, which in molecular chemistry can be arbitrary small and still provide considerable effects. It is clear, that in the given problem global optimization by any method becomes a game of chance. A default strategy of `NMinimize` is first to apply `NelderMead` "downhill simplex" method, and, in the case of poor performance, switch to `DifferentialEvolution`, which is similar to genetic algorithm, and adapted to real number optimization. Alternatively, the user can switch to `RandomSearch`, a multiply restarted local optimizer, for which the user can select between `PenaltyFunction` and `InteriorPoint` constraint minimizers. As a last resort, `SimulatedAnnealing` can be used, which emulates a physical process of a melted metal cooling, asymptotically reaching the globally minimal energy state. For this purpose, an
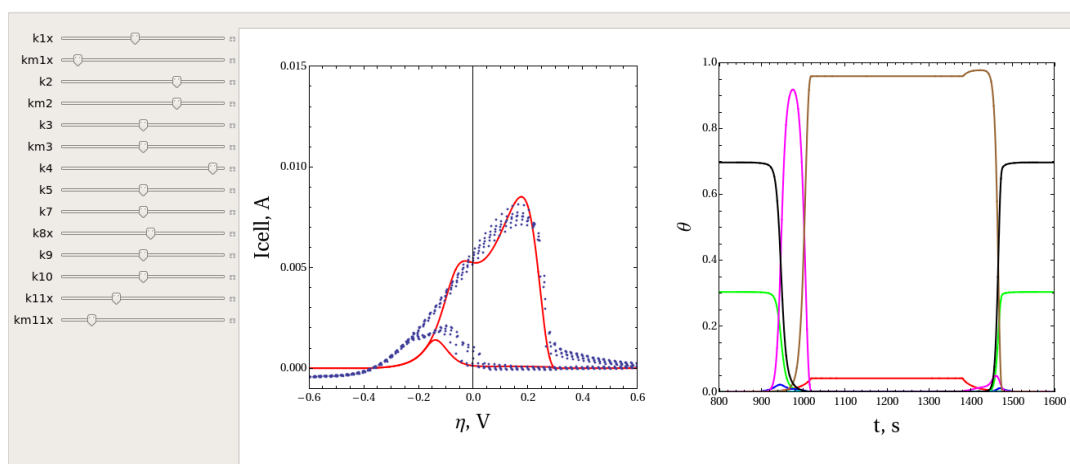
Figure 4: A tool for interactive parameter study. On the left – sliders for variation of parameters, in the center – CV plot, on the right – surface coverage profiles.
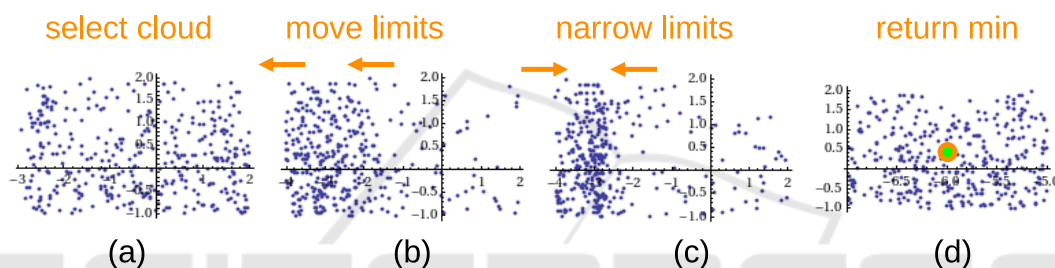
Figure 5: Illustration of Iterative Monte Carlo algorithm.

extremely slow cooling schedule must be used: $T \sim 1/\log t$, here t is time, T is the absolute temperature.

While global optimization methods are considered, also deep local minima are of interest, not only a single global minimum. In our application, NMinimize with default settings requires 5000 iterations and 35 min (on 3 GHz CPU) for convergence. The quality of the minimum is usually comparable with the other methods. However, in the parameter identification problems with several deep local minima of χ^2, all of them may become interesting. Such local minima can reveal hidden discrete symmetries of the problem, or, in our case, can indicate several alternative chemical mechanisms, explaining the same experimental data. Therefore, we have to involve more exhaustive methods for seaching the alternative solutions.

Traditional Monte Carlo, also known as Direct Search method uses a random sampling of parameter space and an iterative strategy of its refinement. For example, one can use the following procedure:

Algorithm (Iterative Monte Carlo)
```
run:  generate N random points
      in specified limits
```

```
select cloud:   χ² < threshold
plot cloud in 2D projections (kᵢ,kⱼ)
if cloud is on the border,
   move limits,
   repeat run
if cloud is localized,
   narrow limits,
   repeat run
return min over the cloud.
```

Fig.5 illustrates the work of the algorithm. On the step (a) the multidimensional cloud $\chi^2 <$ threshold is selected, here presented in a certain (k_i, k_j) projection. The threshold is adjusted to have approximately 500 points in the cloud. The parts (b) and (c) show moving and narrowing steps. At the end of iterations, at step (d), the minimum over the cloud is returned.

In our settings, generation of one population of $N = 120000$ points requires 6 hours (on 3 GHz CPU), and one needs 3-5 iterations for convergence. The advantage of this algorithm is a possibility to branch iterative process towards several solutions and an availability of a large amount of data, representing the behavior of χ^2 in the tested hypervolume. It allows, in particular, to detect the directions, on which χ^2 is almost independent. These directions represent contin-

uous symmetries of the system and will be discussed in details below.

5 RESULTS

Fig.6 shows the results of fitting of experimental CV plot, measured for concentration of *KOH* 0.1M, CH_3OH 0.5M and temperature 300.75K. Generally, for randomly selected point in the space of k-parameters, hysteresis effect is negligible, as shown on Fig.6 left. Hysteresis effect is present only for a thin subset of parameters, complicating additionally the parameter identification procedure.

A simple estimation by the order of magnitude $I_{cell} \sim kFA$ shows that $I_{cell} \sim 10$ mA and $FA \sim 1$ Cl m^2/mol correspond to $k \sim 10^{-3}$ mol/(m^{2}s). The scale of dynamics $\tau \sim C_{act}/k \sim 0.1$ s, characterizing a typical delay in solutions of differential equations, is much smaller than the period $T_p = 800$ s of CV curve. So small delay time cannot lead to the visible hysteresis, therefore, hysteresis becomes a rare effect in parametric space and requires special explanations.

Such behavior can appear near the stationary state with almost degenerate Jacobi matrix. Let eigenvalues of Jacobi matrix J be $|\lambda_{max}| \gg |\lambda_{min}|$, corresponding to a case of stiff system. Note, that eigenvalues λ coincide with the poles in EIS measurements (Clees et al., 2017), while the eigenvectors v are the eigenmodes of the equation $\delta\dot\theta = J\delta\theta$, linearizing our system in the vicinity of the stationary state, $\delta\theta = ve^{\lambda t}$. Note, that $\lambda < 0$ by Lyapunov's stability criterion and that $\tau = 1/|\lambda|$. Thus, small λ correspond to large τ, nearly degenerate systems possess large delay time. This gives an explanation not only for anomalously large hysteresis in CV, but also for slow relaxation to the stationary state in PC analysis and for strong hierarchy in EIS spectra, mentioned in (Clees et al., 2017). In Appendix we give an analytical estimation of the hysteresis effect in linear approximation, showing that the degenerate Jacobian indeed leads to the large hysteresis.

A particular mechanism for origination of the stiff system can be a presence of a reagent, weakly coupled to the rest of reactions, i.e., all reactions involving this reagent have small reaction constants. Although this reagent is weakly coupled, it can occupy free surface of the electrode and influence the dynamics through θ_0-variable, in this way producing hysteresis effect. Looking on the reaction graph on Fig. 1, we see that if this reagent is located in the main chain, such decoupling will break the oxidation process. This will produce the current in the range of microamperes, typical for experimental measurements with pure *KOH* with-

out a fuel. To have simultaneously large current and large hysteresis, the decoupled reagent must be located in one of parallel branches of the reaction graph. Four such places can be identified, shown by orange frames on Fig. 1. Correspondingly, our search procedure also finds four islands of solutions.

Fig.6 center shows the best match results with decoupled reagents CO_{ad} (red solid line, scenario 1) and $COOH_{ad}$ (green dashed line, scenario 2). Scenario 1 shows similarity with experimental CV shape, however, it possesses a sharp shoulder with rapid current variation. This shape is also very sensitive to the variation of reaction constants. In scenario 2 the optimal solution possesses less similarity with the experiment.

Fig.6 right shows the best match results with decoupled *PtO* in reactions r_{11} (green dashed line, scenario 3) and r_{12} (red solid line, scenario 4). These scenarios represent different mechanisms of platinum oxidation and both have a good match with the experiment. The smoother and better matching shape corresponds to sequential mechanism in scenario 4. Table 3 represents the best fit results for all four solutions with their χ^2. For reaction constants their logarithms are given:

$$p_i = \log_{10}(k_i/[mol/(m^2 s)]). \qquad (7)$$

Fig.7 shows one more interesting result, found by the search procedure. It shows the clouds of points with $\chi^2 <$ threshold in projections to (k_1, k_2) and (k_1, k_{11}) planes, in logarithmic scale. Straight lines, visible on these plots show that χ^2 possesses stable minimum in perpendicular direction, but shallow minimum along this line. In other words, the reaction dynamics depends mainly on ratios k_2/k_1, k_{11}/k_1 and only those ratios can be stably determined in the experiment.

6 CONCLUSION

We have presented the methods for parameter identification in cyclic voltammetry of alkaline methanol oxidation. The process involves 11 elementary reactions, 9 main reagents and is described by a system of 6 non-linear differential equations. For parameter identification we use a combination of automatic global optimization methods, traditional Monte Carlo and interactive parameter study. Typically, the integration of the system requires 0.5 sec on 3GHz CPU. Automatic global optimization requires 5000 iterations and 35 min per solution. Monte Carlo generation of one population of 120000 points requires 6 hours and the related iterative algorithm requires 3-5 such populations for convergence.
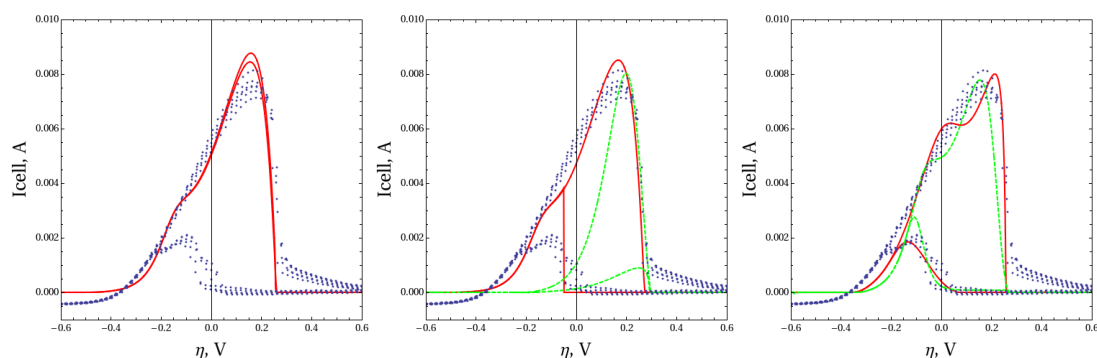
Figure 6: Fitting results. On the left – a typical point with small hysteresis, in the center – optima for scenarios 1 (red solid) and 2 (green dashed), on the right – optima for scenarios 3 (green dashed) and 4 (red solid).

Table 3: The results of the fit.

Log Constants	Scenarios			
	1	2	3	4
p_1^0	0.00563922	-0.943937	-0.547725	0.0522747
p_{-1}^0	-6.79587	-4.02246	-3.94555	-3.94555
p_2	2.15543	1.49158	0.452275	0.752275
p_{-2}	2.17691	0.206631	0.512761	0.512761
p_3	0.867985	0.669569	4.74111	5.04111
p_{-3}	-6.98732	-3.55996	-3.01602	-2.61602
p_4	-6.0547	-1.42416	-0.126364	-1.12636
p_5	-6.80188	-0.920436	0.128806	0.128806
p_7	-0.680335	-2.95533	0.281251	0.281251
p_8^0	-4.45484	-6.6238	-3.64495	-2.64495
p_9	-7.0526	-6.47801	1.79963	1.79963
p_{10}	-2.57335	-12.2244	-1.31402	-1.51402
p_{11}^0	–	–	-4.04773	–
p_{-11}^0	–	–	-6.29566	–
p_{12}^0	–	–	–	-4.84773
p_{-12}^0	–	–	–	-6.09566
$\chi^2/[A^2]$	0.000170361	0.00102207	0.000332658	0.000161844

As a result of our parameter study, we have found 4 optima corresponding to different mechanisms of the underlying chemical process. All scenarios introduce a reagent, weakly coupled to the rest of the reactions and differ by selection of this reagent. The weakly coupled reagent has slow kinetics, on the other hand it occupies free electrode surface and is able to block the cell current. In this way it produces the hysteresis effect observable in experimen-

tal plots, being slowly accumulated in the increasing voltage phase and slowly reduced in the decreasing one. The weak coupling of the reagent is also responsible for high condition number of the system matrix, leading to slow convergence of experimental polarization curves and strong hierarchy of electroimpedance spectra.

The best match for every scenario is presented and the details of the related kinetics are discussed.
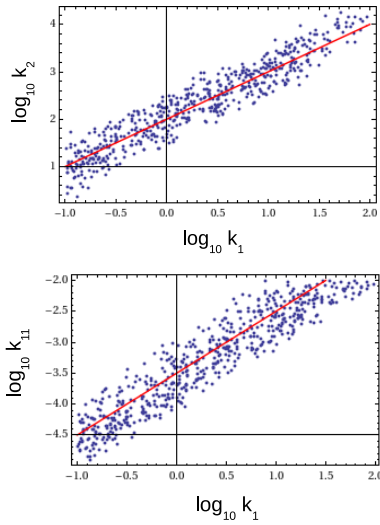
Figure 7: Correlation of parameters k_1, k_2 and k_{11}.

REFERENCES

Bard, A. J. and Faulkner, L. R. (2000). *Electrochemical Methods: Fundamentals and Applications*. Wiley.

Bäck, T. (1996). *Evolutionary Algorithms in Theory and Practice*. Oxford University Press, New York.

Beden, B. et al. (1982). Oxidation of methanol on a platinum electrode in alkaline medium: effect of metal ad-atoms on the electrocatalytic activity. *J. Electroanalytical Chem.*, 142:171–190.

Ciucci, F. (2013). Revisiting parameter identification in electrochemical impedance spectroscopy: Weighted least squares and optimal experimental design. *Electrochimica Acta*, 87:532–545.

Clees, T. et al. (2014a). Focused ultrasonic therapy planning: Metamodeling, optimization, visualization. *J. Comp. Sci.*, 5(6):891–897.

Clees, T. et al. (2014b). Quasi-Monte Carlo and RBF Metamodeling for Quantile Estimation in River Bed Morphodynamics. In Obaidat, M. S. et al., editors, *Simulation and Modeling Methodologies, Technologies and Applications, Advances in Intelligent Systems and Computing 319*, pages 211–222. Springer.

Clees, T. et al. (2017). Electrochemical Impedance Spectroscopy of Alkaline Methanol Oxidation. In *Proc. INFOCOMP 2017, The Seventh International Conference on Advanced Communications and Computation*, pages 46–51. IARIA.

Gamry Instruments (2018). Basics of Electrochemical Impedance Spectroscopy. http://www.gamry.com/application-notes/EIS/basics-of-electrochemical-impedance-spectroscopy. Online tutorial.

Griffiths, P. and de Hasseth, J. A. (2007). *Fourier Transform Infrared Spectrometry*. Wiley-Blackwell.

Ilonen, J. et al. (2003). Differential Evolution Training Algorithm for Feed Forward Neural Networks. *Neural Proc. Lett.*, 17:93–105.

Krewer, U. et al. (2006). Impedance spectroscopic analysis of the electrochemical methanol oxidation kinetics. *Journal of Electroanalytical Chemistry*, 589:148–159.

Krewer, U. et al. (2011). Electrochemical oxidation of carbon-containing fuels and their dynamics in low-temperature fuel cells. *ChemPhysChem*, 12:2518–2544.

Mathematica 11 (2018). Reference Manual. http://reference.wolfram.com.

Nikitin, I. et al. (2012). Stochastic analysis and nonlinear metamodeling of crash test simulations and their application in automotive design. In Browning, J. E., editor, *Computational engineering: design, development, and applications*, pages 51–74. Nova Science.

Otten, R. H. J. M. and van Ginneken, L. P. P. P. (1989). *The Annealing Algorithm*. Kluwer.

Press, W. H. et al. (1992). *Numerical Recipes in C: Chap. 15*. Cambridge University Press.

Strutz, T. (2016). *Data Fitting and Uncertainty: A practical introduction to weighted least squares and beyond*. Springer.

Wächter, A. and Biegler, L. T. (2006). On the implementation of an interior-point filter line-search algorithm for large-scale nonlinear programming. *Mathematical Programming*, 106:25–57.

APPENDIX: LINEAR ESTIMATION OF HYSTERESIS EFFECT

Consider a system of differential equations:

$$C_{act}\, \theta' = f(\theta, \eta) \tag{8}$$

in the limit $C_{act} \to 0$. In this way we emulate the systems with small delay time $\tau = C_{act}/k \to 0$.

The solution is located in the vicinity of the stationary curve

$$f(\theta^*, \eta) = 0, \tag{9}$$

where both θ^* and η depend on t. After differentiation, we have

$$J\theta^{*\prime} + \frac{\partial f}{\partial \eta}\eta' = 0, \quad J = \frac{\partial f}{\partial \theta}. \tag{10}$$

Further, in linearized equations

$$C_{act}(\theta^{*\prime} + \delta\theta') = f(\theta^*, \eta) + J\delta\theta, \tag{11}$$

omitting small $\delta\theta'$ term and using (9) and (10), we have

$$\delta\theta = -C_{act}J^{-2}\frac{\partial f}{\partial \eta}\eta'. \tag{12}$$

Substituting it to the linearized expression for current, we obtain

$$\delta I = \left(\frac{\partial I}{\partial \theta}\right)^T \delta\theta = \tag{13}$$

$$-C_{act}\left(\frac{\partial I}{\partial \theta}\right)^T J^{-2}\left(\frac{\partial f}{\partial \eta}\right)\eta'.$$

As a result, we see, that a deviation of current from the stationary curve changes sign with η', i.e., possesses the hysteresis effect. In general position, the vectors on the left and on the right of J^{-2} in (13) do not coincide with annulators of Jacobian, i.e., its left and right eigenvectors with tending to zero eigenvalue. In this case, the amplitude of hysteresis effect tends to infinity, in the limit when the Jacobian becomes degenerate:

$$\det J \to 0, \ \delta I \to \infty. \tag{14}$$

This condition can be used only as an indicator of hysteresis effect. With increasing δI, one will need to apply the next order corrections to approximate its value.